Concurrent elution of calcium phosphate and macromolecules from alginate/chitosan hydrogel coatings

Ping Peng[a)]
Ian Wark Research Institute, University of South Australia, Mawson Lakes, Adelaide, South Australia 5095, Australia

Nicolas H. Voelcker
School of Chemistry, Physics and Earth Sciences, Flinders University, G.P.O. Box 2100, South Australia 5042, Australia

Sunil Kumar and Hans J. Griesser
Ian Wark Research Institute, University of South Australia, Mawson Lakes, Adelaide, South Australia 5095, Australia

(Received 15 July 2008; accepted 17 November 2008; published 2 February 2009)

The concurrent release of calcium phosphate and biomacromolecules may improve wound healing responses at the interface with ceramic materials of orthopaedic and dental implants. Hydrogel coatings consisting of a mixture of alginate and chitosan were doped and applied onto solid carriers with the aim of investigating their use as local delivery vehicles. Coatings containing both the model macromolecule FITC-dextran 70 kDa (FD 70) and dispersed calcium phosphate carbonate (CPC) nanoparticles were coated onto a solid, nonporous model substrate to study the concurrent release of FD 70 and calcium and phosphate ions from within the hydrogel. Hydrogel coatings containing only FD 70 were cast onto porous calcium phosphate coatings, similar to hydroxyapatite, to study the release of FD 70 from, and calcium and phosphate ions through, the hydrogel coating. Transmission electron microscopy showed good dispersion of the CPC nanoparticles, and scanning electron microscopy and atomic force microscopy showed that increased CPC loading resulted in an increase in surface roughness but to extents well below those affecting cell responses. The release of FD 70 from CPC-loaded coatings was similar to release from the hydrogel alone, although higher CPC loadings resulted in small changes. The release of FD 70 was better described by double or triple phase zero order release kinetics; this complex time dependence indicates that in addition to outdiffusion, other, time-dependent factors apply, such as swelling of the gel, as expected from the known effects of calcium ions on alginate. Calcium and phosphate ions were also released, with similar release kinetics, through the hydrogel layer from the underlying CaP layer. In either case, release decreased to negligible levels after 3 days, suggesting that the systems of this study are suitable for short-term concurrent release of water-soluble biomacromolecules and calcium and phosphate ions. © *2008 American Vacuum Society.* [DOI: 10.1116/1.3046123]

I. INTRODUCTION

The surface composition and associated properties are key determinants for the successful integration of implants into biological tissues. A central strategy in the development of biomedical devices is to create biomimetic surfaces for directing the biological responses following implantation.[1] Toward this aim, one strategy is the local delivery of specific biologically active molecules such as extracellular matrix adhesion proteins, growth factors, cytokines, and antibacterials, directly at the implant/tissue interface in order to elicit predictable, targeted local host responses.[2] Therefore, there has been increased interest in the use of eluting coatings in combination with well-established endoprosthetic bulk biomaterials such as metallic or plastic orthopaedic implants.[3–8] In comparison with bulk delivery systems, the use of release coatings on solid biomaterials possesses the advantage of allowing independent design of the coating and the underlying material in order to satisfy other required criteria such as bulk mechanical strength.

In previous work, we developed eluting coatings based on a mixed alginate/chitosan hydrogel containing dissolved macromolecules.[9] Such hydrogel coatings could be used for the local release of, for instance, growth factors. To explore their potential use for application for tooth and bone prosthetic devices, we then aimed to investigate how the release of biomacromolecules could be combined with the release of inorganic ions, particularly calcium and phosphate; this is the subject of this report. Calcium phosphate based ceramics are widely used in tooth and bone prosthetic devices due to their similarity to naturally occurring apatite. Although the exact mechanisms responsible for their good biocompatibility are still the subject of intense investigation, it has been shown that calcium phosphate ceramics undergo resorption, subsequent remodeling, and biomineralization.[10–15] More specifically, it is the increased local concentration of calcium and

[a)]Author to whom correspondence should be addressed; Present address: Molecular and Health Technologies, CSIRO, Bag 10, Clayton South MDC, VIC 3169, Australia; electronic mail: ping.peng@csiro.au

phosphate ions from the resorbing calcium phosphates that is considered to be conducive to new bone formation.[16]

The concurrent release of calcium and phosphate ions as well as bioactive molecules such as growth factors may offer additional possibilities for the control of orthopaedic wound healing. However, the question arises whether application of a macromolecule-containing hydrogel coating onto a calcium phosphate substrate might lead to reduction in the calcium and phosphate release. Another question of interest was whether one might be able to release concurrently biomacromolecules and calcium and phosphate ions from the same hydrogel coating, which would be of interest for the coating of hard tissue implants without the need for a separate HA coating. With this in mind, we have investigated two different designs of nanocomposite eluting coatings based on alginate/chitosan hydrogels.

In one design, we dispersed both a model biomacromolecule (FITC-dextran) and calcium phosphate nanoparticles within the hydrogel matrix, which was cast onto a solid, nonporous substrate, with the aim of concurrent release upon swelling of the hydrogel matrix in an aqueous medium. Calcium phosphate carbonate (CPC) was used as the source of calcium and phosphate ions as it is similar to the mineral phase in teeth and bones, which is calcium phosphate based and contains some CO_3^{2-} ions. Upon partial substitution of either PO_4^{3-} or OH^- by CO_3^{2-}, the crystal size of precipitated calcium phosphate was found to be reduced by approximately an order of magnitude.[17–19] The resultant smaller nanoparticles are better suited to dispersion in a thin coated hydrogel layer.

In the alternative design, FITC-dextran was loaded within an alginate matrix, which was cast onto, and into the pores of, a porous calcium phosphate coating. An electrochemically deposited calcium phosphate coating[20] was used as a model porous orthopaedic surface, because commercial hydroxyapatite samples were too rough for our experiments. Calcium and phosphate ions were expected to dissolve from the base layer and diffuse through the alginate/chitosan layer upon interaction with an aqueous medium.

In both these designs, the aim is to locally deliver bioactive molecules as well as calcium and phosphate ions for improved integration of orthopaedic implants. There has been considerable recent interest in the use of alginate or chitosan hydrogel coatings, sometimes with dispersed calcium phosphate particles, for orthopaedic and periodontal implants as well as nerve regeneration.[21–34] The concurrent release of active biomacromolecules may provide additional means of directing biological responses to implants, but prior to the design of clinical investigations it is essential to acquire *in vitro* data, and understand the performance and limitations of the release system. Thus, we here characterize the release behavior and release rates of both macromolecules and inorganic ions from or through hydrogel coatings, after detailed chemical, structural, and morphological characterizations of the coatings and the embedded nanoparticles by a range of analytical techniques.

II. MATERIALS AND METHODS

A. Synthesis of calcium phosphate carbonate powder

Calcium phosphate carbonate was prepared as described by Rey *et al.*[18] The calcium ion solution containing 17.7 g $Ca(NO_3)_2 \cdot 4H_2O$ in 250 ml water was quickly mixed with 500 ml phosphate solution containing 20 g $(NH_4)_2HPO_4$ and 20 g $(NH_4)_2CO_3$ as well as 40 ml ammonia solution at room temperature. The precipitate was immediately filtered through "medium fast qualitative" filter paper (Whatman), washed by Milli-Q water and lyophilized for 24 h.

B. Calcium phosphate coatings on Ti substrates by electrochemical deposition

Electrochemical deposition of calcium phosphate coatings on titanium (Ti) substrates was carried out as described earlier.[20] Briefly, titanium substrates (99.7%, Aldrich Chemical Co.) with an area of 4 cm^2 and 0.25 mm thickness were cleaned by ultrasonication in acetone, rinsing in Milli-Q water and soaking in ethanol overnight (12 h), followed by a final rinse in Milli-Q water. Calcium phosphate coatings were deposited on both sides of the substrate by electrochemical deposition. The electrochemical setup consisted of a three-electrode configuration with the titanium substrate as the working (cathode) electrode ($20 \times 20 \times 0.25$ mm^3), two platinum counter electrodes ($25 \times 25 \times 0.1$ mm^3) and a saturated calomel electrode (SCE), which was used as the reference electrode. A periodical pulsed potential at 0.3 Hz, 2500 ms, and 2.2 V was applied to the working electrode via a potentiostat (AD Instrument) for 20 min. The SCE was located close (1–2 mm) to the titanium electrode through a Haber-Luggin capillary salt bridge. The deposition was carried out while continuously stirring the electrolyte solution, held at 37 °C with the aid of a water bath. Calcium phosphate coated samples were immediately removed from the electrolyte solution, washed in Milli-Q water and dried under a stream of compressed air. Chart software (AD Instrument) was used to control the potentiostat.

C. Hybrid hydrogel: Incorporation of CPC in alginate hydrogel

The hybrid hydrogel was made by mixing CPC powder into 2.2% alginate solution (alginic acid, sodium salt, from the kelp Macrocystis pyrifera, Sigma-Aldrich Corporation) at percentage values of 1%, 2%, or 3% (w/w). After stirring for 2 min, the mixture was ultrasonicated for 30 min, then allowed to stand overnight at room temperature. The semitransparent gel, termed hybrid hydrogel, was then separated from the precipitate by decanting with the aid of a syringe and stored at 4 °C until further use. The analysis of the hybrid hydrogel by inductively coupled plasma optical emission spectroscopy determined the final calcium phosphate carbonate concentrations to be 0.3%, 0.5%, and 1.0% (w/w).

D. Loading of macromolecules

Fluorescein isothiocyanate dextran (FITC-dextran) with an average molecular weight (MW) of 71 600 Da (FD 70, Sigma-Aldrich Corporation) and polydispersity 1.29, used as a model release molecule for the present study, was added to 2.2% sodium alginate solution or the hybrid CPC-loaded hydrogel at a weight ratio of 1:12.

E. Preparation of eluting coatings

Alginate/chitosan/and alginate/chitosan/CPC composite coatings were prepared on cellulose nitrate filter paper (0.45 μm, Sartorius, Germany), used here as a porous model substrate intended to mimic the rough and porous nature of commercial hydroxyapatite coatings and other implant materials onto which hydrogel coatings might be applied. Filter paper samples were cut to 9 cm^2 in size and fixed on a glass substrate of exactly the same size by double-sided sticky tape. 1.5 ml hybrid hydrogel was then spotted on to fully cover the filter paper, followed by spinning at a rate of 5500 rpm for 7 s unless otherwise stated. After drying at room temperature, the coated sample was immersed in 1*M* $CaCl_2$ for 3 min; afterwards, it was quickly removed and dipped into 30 ml fresh Milli-Q water once. After careful blotting with Kimwipes® tissue to remove excess water, it was then left to stand on a level bench until dried again. Next, it was soaked in 0.5% chitosan solution for 9 min, followed by dipping twice in 30 ml fresh Milli-Q water. After drying again on a level bench at room temperature (around 10 min) to achieve a constant weight within 0.2 mg accuracy, the samples were stored in a plastic box for 10 days, sealed with aluminum foil and kept at 4 °C.

Alginate/chitosan/CPC composite coatings were also coated onto silicon wafer substrates. Silicon wafers (P/boron doped, [100], one side polished, 475–575 μm thick, Micro Materials & Research Consultancy Pty. Ltd., Australia) were cut to 7×12 mm^2 size, washed in acetone, rinsed in Milli-Q water, soaked in 5% NaOH for 5 min, briefly dipped into Milli-Q water, transferred into 2*M* HCl solution for 1 min, then rinsed with Milli-Q water and dried under a stream of compressed air for immediate use. They were initially spin coated with 20 μl of a 0.25% chitosan solution (chitosan >85% deacetylated, Sigma-Aldrich Corporation) at a speed of 5500 rpm for 9 s, then quickly dried while the spinning continued. The procedure for preparation of alginate/chitosan/CPC composite coatings additionally loaded with FD 70 was similar to that on the filter paper substrates but using 100 μl of hybrid solution. Subsequently, chitosan layers were spin coated onto the dried alginate outer layer on a leveled spinner, by spotting 100 μl of a 0.5% chitosan solution onto the sample and incubating for 9 min. Finally, the sample was spun at a speed of 5500 rpm for 9 s. The remainder of the procedure was the same as that used for the paper substrate.

Alginate/chitosan blend coatings loaded with FD 70 on electrochemically deposited calcium phosphate coatings on Ti substrates were prepared in the same way as used for silicon wafer substrates, except replacing the hybrid hydrogel with alginate solution containing FD 70.

F. Analysis of dispersion of CPC powders in alginate hydrogels

Hybrid hydrogel films containing different percentages of calcium phosphate carbonate powders were prepared by dipping 3 mm Cu transmission electron microscopy (TEM) grids into the hybrid hydrogel bulk and allowing the entrapped water of the hybrid hydrogel to evaporate in air. Both 200 mesh and 400 mesh grids were used. The film thickness was estimated to be in the range of 50–150 nm. The composite hydrogel films were coated with a thin layer (approximately 3 nm) of carbon to make the samples electrically conducting for TEM examination. The films were examined on Philips CM100 and CM200 transmission electron microscopes. The CM100 was used for primary imaging of the hydrogel films and was operated at an accelerating voltage of 80 kV. The CM200 was fitted with an EDAX DX 4 energy dispersive x-ray (EDX) system and was used for elemental analyses of the composite hydrogel films. The CM200 was operated at an accelerating voltage of 200 kV.

G. Morphology of the composite coatings

The morphology of hydrogel coatings on silicon wafers was examined with a field emission scanning electron microscopy (SEM) (Philips XL30), operating at an acceleration voltage between 5 and 10 kV. Samples were coated with carbon prior to analysis. EDX was also conducted for elemental identification.

Atomic force microscopy (AFM) (Digital Instruments Nanoscope III Multimode microscope) imaging was conducted under ambient conditions in air using tapping mode with an etched silicon probe (model TESP). Image processing was performed using WSXM 3.0 BETA 6.5 software (Nanotec Electronica S.L.). Roughness was measured as rms and height histograms plotted using the roughness analysis routine in WSXM 3.0 BETA 6.5. The number of intervals was fixed at 120 and the minimum (beginning of the interval) and maximum heights (end of the interval) were constrained at 0 and 180 nm, respectively.

μ-TA measurements were conducted using a 2990 Micro Thermal Analyzer (TA Instrument), where the surface image was obtained by monitoring the electrical power required to maintain a constant tip temperature while the tip is rastered on the surface of the sample under investigation. The image contrast is determined by the heat flow from the tip to the surface, mapping relative differences in thermal conductivity across different materials on the sample surface. Localized thermal analysis (LTA) was probed on individual locations on the surface, using the thermal probe as a tiny thermal analyzer. As the probe heats the sample at a rate of 10 °C/s from room temperature to 455 °C, expansion or softening can be measured by the movement of the laser signal on the photodetector, which is analogous to conventional thermomechanical analysis (TMA).[35]

The thickness of the films was measured using ellipsometry (Beaglehole Instruments), with ten different incident angles on the sample, a wavelength of 600 nm, a refractive index of the silicon wafer of 3.95,[36] and assuming an initial refractive index of the film of 1.53.[37]

H. Surface chemistry of the composite coatings

X-ray photoelectron spectroscopy (XPS) measurements were performed on a Physical Electronics PHI 5600 ESCA system (software: AUGER SCAN, version 2.41) with a nonmonochromatic Mg $K\alpha$ x-ray source ($h\upsilon$=1253.6 eV) at a base pressure of $<10^{-8}$ Torr and an accelerating potential at 15 kV. The photodetector take-off angle (defined as the angle between the surface normal and the axis of the analyzer) was 45° unless stated otherwise. The binding energy E_b scales were corrected for sample charging by setting the C 1s E_b of adventitious carbon to 284.6 eV. A survey spectrum was recorded using a pass energy of 93.9 eV to determine the elemental compositions of the surface. High-resolution spectra in multiplex mode were recorded from individual peaks at 23.5 eV pass energy.

A Nicolet FTIR (Magna-IR™ spectrometer 750), equipped with a liquid nitrogen cooled, broadband mercury cadmium telluride detector and a diffuse reflectance cell (Spectra Tech), was used to measure IR spectra under a stream of N_2 at a flow rate of 40 cm^3/s, with a total of 160 scans and a resolution of 4 cm^{-1} and a mirror velocity of 0.6329 cm/s. Potassium bromide was used as a reference for background subtraction and diluent for calcium phosphate carbonate powders for analysis, while bare silicon wafers were used as a reference for hydrogel coatings on silicon wafers.

I. Release

Simulated body fluid (SBF) was used as the release medium in the present study: 1.67 mM of K_2HPO_4, 2.5 mM of $CaCl_2$, and 137.8 mM of NaCl in Milli-Q water were adjusted to pH 7.2 by addition of 50 mM of tris(hydroxymethyl)aminomethane $[(CH_2OH)_3CNH_2]$ and 1M hydrochloric acid. The release of FD 70 was assessed by measuring the fluorescence intensity from FD 70 using a luminescence spectrometer (Perkin-Elmer LS 55). Coatings on silicon wafers or calcium phosphate coated titanium (7×12 mm^2) were soaked in 3 ml SBF at 37 °C with slow stirring, while measuring the fluorescence intensity (E_x/E_m: 490/517 nm for FITC-dextran, at the same slit width of 5 nm) in time-lapse mode. Otherwise, they were kept in a shaking incubator at 37 °C and 95 rpm. To calculate the percentage of released FD 70, the total release (100%) was estimated by immersing the samples immediately after spin coating into 3 ml phosphate buffered solution (pH=7.4) and measuring the fluorescence after 7 d storage at 4 °C.

The release of calcium and phosphate ions was measured using inductively coupled plasma optical emission spectroscopy (ICP-OES) (Optima 3000 ICP-OES instrument, Perkin-Elmer). The alginate/chitosan/calcium phosphate carbonate composite coatings on paper with a square area of 9 cm^2 or alginate/chitosan blend layers on calcium phosphate coatings on Ti with a square area of 4 cm^2 were soaked in 10 ml of SBF at pH 7.2 for time intervals of 1, 2, 3, 6, 9, 28, and 37 days, respectively. At each scheduled interval, 0.5 ml solution was taken out and diluted to 10 ml in a volumetric flask with 0.02 N HCl for analysis, while adding 0.5 ml of fresh SBF into the test solution to keep the volume of release medium constant at 10 ml. On day 28, 0.5 ml of 0.02M HCl was added to the test solution to keep the volume of release medium constant at 10 ml and the pH around 6.0. The entire solution on day 37 was used for analysis. The difference of the calcium or phosphate ions from that in the original SBF was used to estimate the amount of ions released from the coatings.

The testing of release model fits is based on linear regression analysis[38] of the transformed release data derived from the corresponding model. In particular, if a nonlinear model was readily available for better fitting, transformation of the release data was made to create a linear graph, and then linear regression was used to analyze this transformed data. Analysis of variance (ANOVA) was used to test the acceptability of release models from a statistical perspective according to the significant value of the F statistic at a level of 0.05. If the value of F is less than 0.05, the linear model is a good fit to the data sets. In addition, the regression for the release accounted for by the model and the residual that is not accounted for by the model were also used to evaluate the acceptability of the model. Furthermore, the strength of the relationship between the model and experimental release profile was assessed via the multiple correlation coefficient R.[39] A large value indicates a strong relationship, and R^2 indicates the fraction of the release data consistent with the model.

III. RESULTS

A. Dispersion of CPC powder in alginate hydrogels

Important determinants of the morphology of the CPC-loaded hydrogel coating, and presumably of the release of calcium and phosphate ions, are the size of the nanoparticles and their aggregation within the hydrogel matrix. Accordingly, we studied these properties by transmission electron microscopy. The size of the CPC particles in the alginate hydrogel was found to be in the range from a few nanometers up to 250 nm. Figure 1 shows representative TEM images for an alginate hydrogel impregnated with 0.5% and 1.0% (w/w%) CPC powder, respectively. More particles are visible for the sample with the higher concentration of 1.0% CPC [Fig. 1(b)] than that with 0.5% CPC [Fig. 1(a)]; however, both preparations also showed agglomerated nanoparticles dispersed in the hydrogel matrix (Fig. 1). EDX analysis showed characteristic signals for Ca and P on the spots with large agglomerates [Fig. 1(c)], whereas no significant signals for these elements were detected for the other regions [Fig. 1(d)].

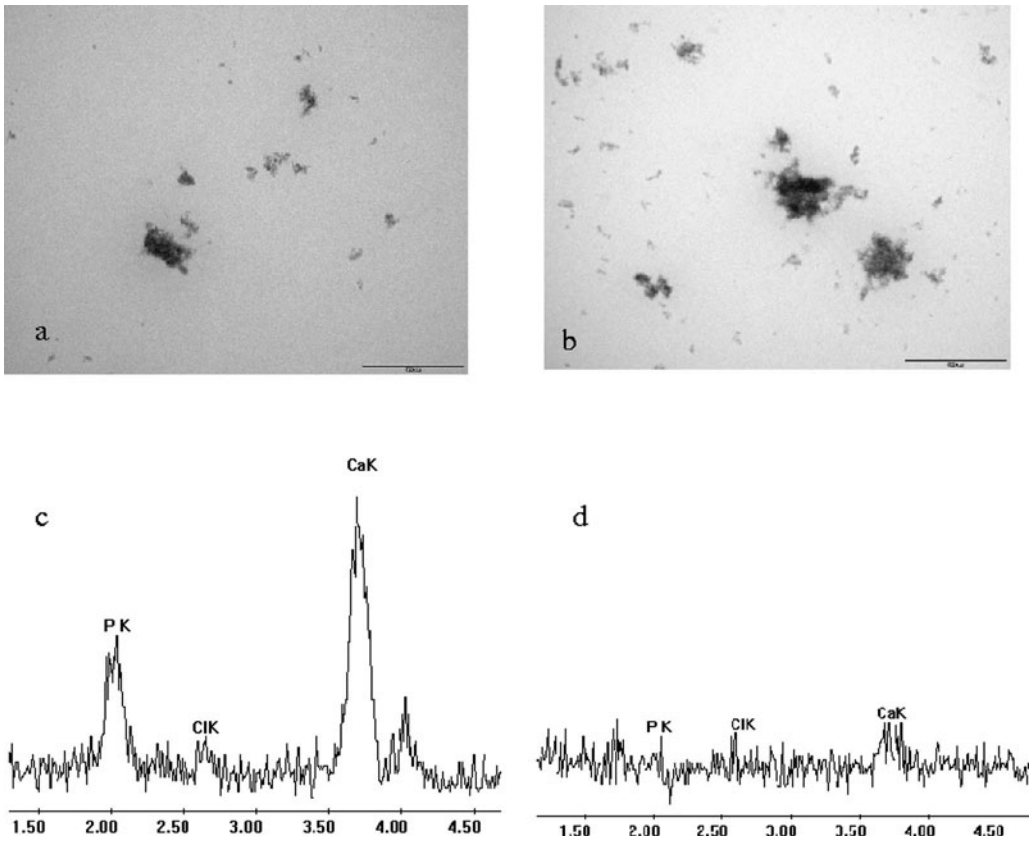

FIG. 1. TEM images and EDX spectra of alginate hydrogel impregnated with CPC powder; (a) hydrogel with 0.5% CPC; (b) hydrogel with 1.0% CPC. (c) EDX spectrum of spot with large cluster of CPC; 1.0% loading. (d) EDX spectrum on a region without CPC clusters. Scale bar: 500 nm.

Another question was whether the incorporation of the nanoparticles and their aggregation would lead to substantial increases in the topology/surface roughness of the hydrogel coatings. SEM images recorded with alginate/chitosan/CPC composite coatings and pure alginate/chitosan blend coatings on Si wafer substrates all displayed a similarly smooth surface, indicating that the surface roughness did not change measurably. Incorporation of the nanoparticles did, however, increase the thickness of the resultant coating. Ellipsometry and cross-section SEM images yielded a thickness value of ~240 nm for the composite coating with 1.0% CPC powder and ~120 nm for the undoped alginate/chitosan blend coating. As alginate is cross-linked with calcium ions, the hybrid hydrogels have a higher viscosity than the pure hydrogel, and this is the likely reason for the increased thickness of the spin-coated doped films. This was observed only qualitatively as rheology was not available; however, as shown below, the release behavior does not change much upon incorporation of the nanoparticles, and hence it was not considered important to quantify the viscosity.

AFM was also used to study the nanoscale topography and morphology of the coatings. Surface roughness values and average heights of 100 μm^2 images are listed in Table I. The rms roughness of the composite coatings at 0.3% CPC was measured to be almost the same as that of the alginate/chitosan blend coatings, whereas increased incorporation of CPC above 0.5% raised the rms values to around four times that of the alginate/chitosan coatings. In addition, the average heights of composite coatings of CPC above 0.5% were almost double compared to that of the alginate/chitosan blend coatings. Yet, compared to the thickness of the coatings and the size of the dispersed CPC nanoparticles, the increases in surface roughness are small, consistent with the SEM observations.

B. Microthermal analysis of coatings

Microthermal analysis provides both imaging and analytical capabilities with submicron spatial resolution for both surface and subsurface details.[35,40,41] With a hydrogel coating thickness of the order of 100 nm, μ-TA is expected to detect

TABLE I. Roughness analysis of blend/composite hydrogel coatings.

	Blended hydrogel coatings	Composite hydrogel coatings		
	Alginate/chitosan	0.3% CPC	0.5% CPC	1.0% CPC
rms, nm	3.0	3.3	13.1	12.4
Average heights (nm)	8.6	10.4	17.9	17.7

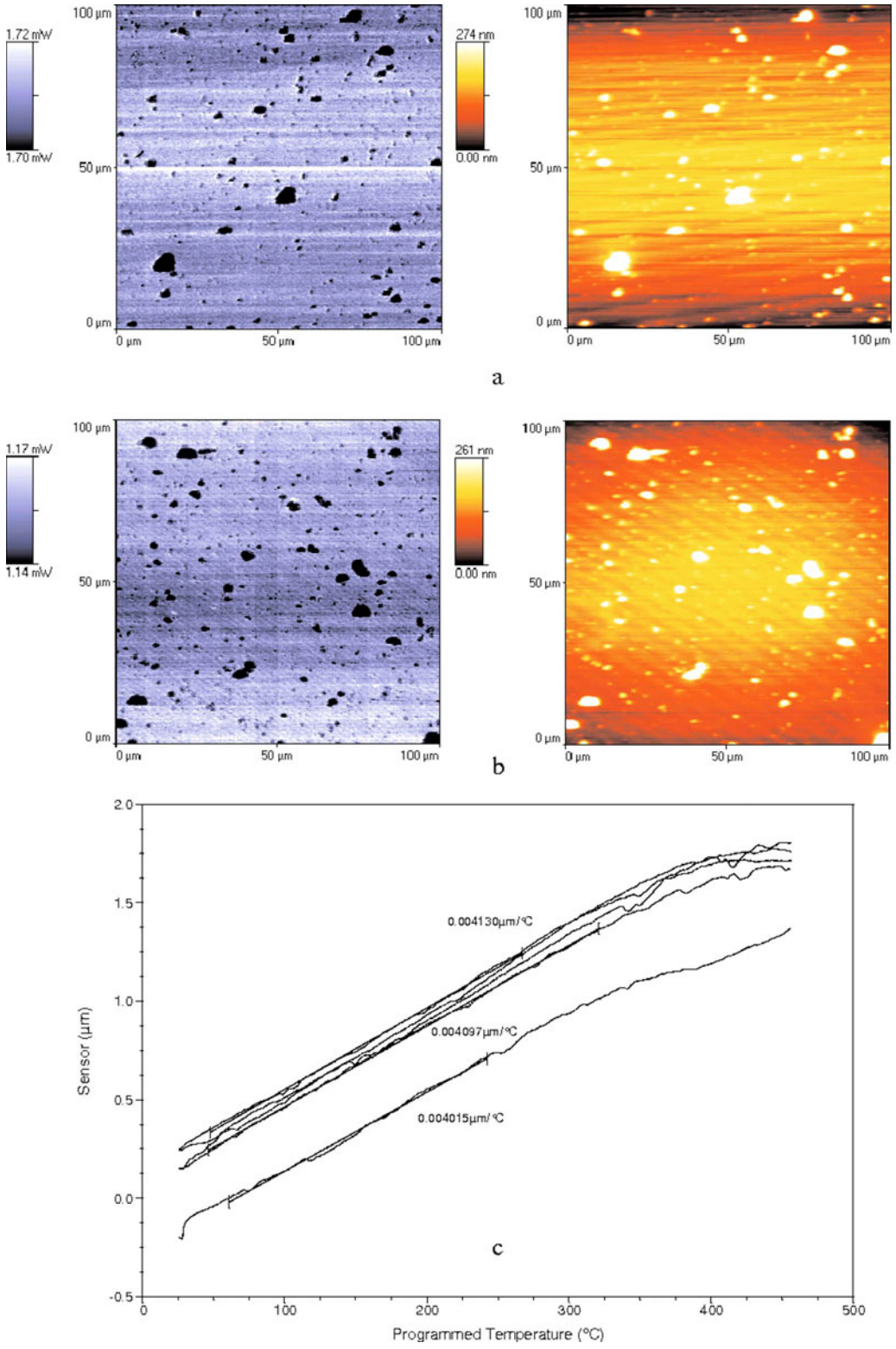

FIG. 2. Imaging and local thermal analysis of composite coatings on silicon wafers by microthermal analysis; (a) 0.5% CPC; (b) 1.0% CPC; (c) 0.5% CPC, local thermal analysis at five different spots.

the thickness-averaged properties of hydrogel coatings. Typical microthermal conductivity and topography images recorded on composite coatings with 0.5% and 1.0% of CPC powder were very similar as shown in Figs. 2(a) and 2(b). The "dark spots" in the thermal images are not from phase differences but from topographic features, as they all correspond very well to the elevated areas in the topographic images. This is because when the probe is at the top of the "mountains," it is surrounded by less materials and more air than when it is on the "plain." Air has a lower thermal con-

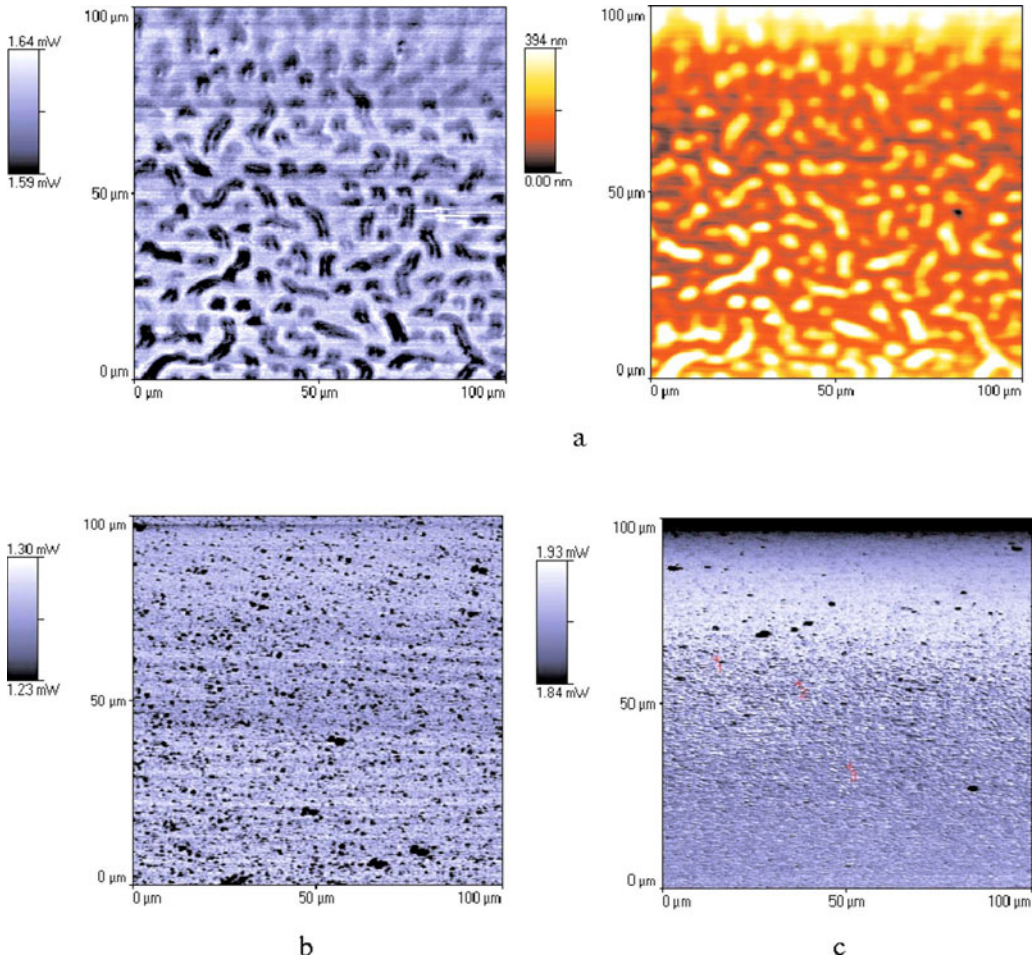

FIG. 3. Images of coatings on silicon wafers by microthermal analysis. (a) Thermal and topography images of alginate layer cross-linked by $CaCl_2$. (b) Thermal image of alginate/chitosan blend coatings. (c) Thermal image of an alginate layer.

ductivity than the sample; therefore, the apparent thermal conductivity measured by the probe is lower.

There are two possibilities for the dark regions in the thermal images. One may relate to the impregnated CPC powder within the hydrogel. Another may be from gel clumps as occasionally observed in SEM. In the first step for cross-linking by $CaCl_2$ solution, the cast alginate layer on silicon wafers was observed to wrinkle and displayed a rough surface with lots of dark areas [Fig. 3(a), left] in the form of gel clumps, which again corresponded very well to the elevated areas in the topography images [Fig. 3(a), right]. On cross-linking by chitosan, alginate/chitosan blend coatings displayed a significantly smoother surface [Fig. 3(b)], which, however, contained more dark areas compared to pure alginate film [Fig. 3(c)] on silicon wafers. These dark areas again were due to topographic features, as they all were also observed in the corresponding topography images. With the inclusion of CPC in the hybrid hydrogel, the gel viscosity increased compared to pure alginate, and as a result, gel clumps might form more readily. As the preparation process of hybrid hydrogels should discard all the CPC particles with a size larger than a micron, as indicated in TEM images, we assume that these dark areas are from gel clumps.

Composite coatings with 0.5% and 1.0% CPC powder content had similar linear sensor slopes [analogous to TMA, Fig. 2(c)] regardless of the location on the surface in LTA analysis, which provided additional evidence that there is no phase separation on the surface of the composite coating. The combined image and LTA analyses suggest that CPC particles are well dispersed within the hydrogel matrix. This is in accord with the results from SEM, EDX, and AFM.

The linear slope in LTA analysis is indicative of a fairly hard surface that causes the tip to retract due to the force-feedback loop of the microscope in dc mode.[35,42] The average thermal expansion coefficient was measured to be 0.0041 ± 0.0001 μm/°C, similar to that of the pure alginate hydrogel matrix, which was 0.0040 ± 0.0004 μm/°C.

C. Chemical analysis of composite coatings

XPS survey spectra of composite coatings with 0.5% and 1.0% CPCs were identical to XPS spectra of undoped alginate/chitosan coatings on silicon wafer substrates.[9,43] The absence of significant intensities of Ca 2*p* and P 2*p* signals in survey spectra and high resolution scans of composite coatings with 1.0% CPC indicates that the incorporated CPC

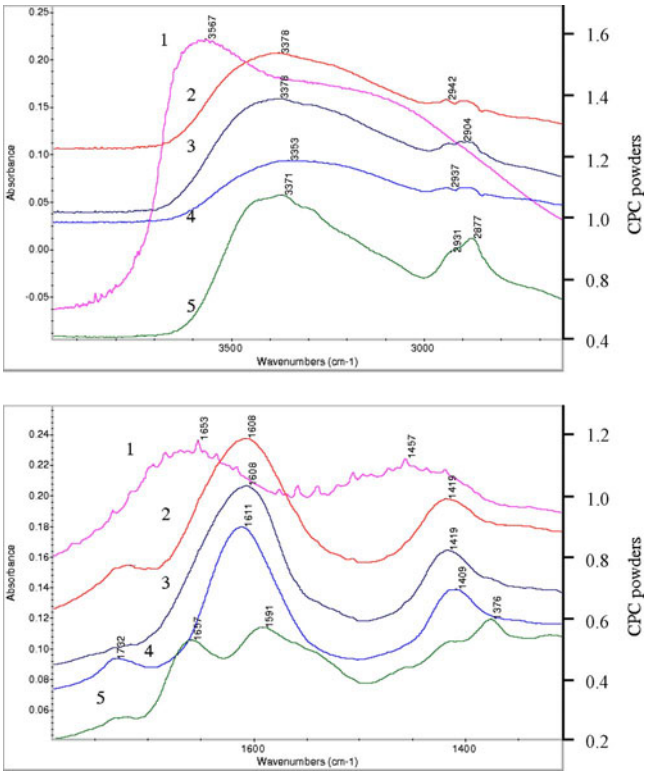

FIG. 4. Drift spectrum of (1) CPC powder; (2) alginate/chitosan layer with 1.0% CPC; (3) alginate/chitosan layer; (4) alginate layer; (5) Chitosan layer.

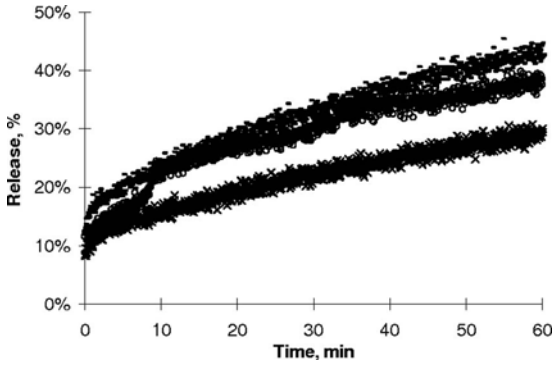

FIG. 5. Release of FD 70 into SBF from composite coatings on silicon wafers containing different percentages of CPC; (1) 0.3% CPC (×); (2) 0.5% CPC (○); (3) 1.0%CPC (■).

powder was embedded in the hydrogel without substantial protrusions, in accordance with the above findings, and near-surface particles were covered with a layer of hydrogel at least 10 nm thick, thus exposing only hydrogel to the air interface. This probably is a consequence of surface free energy. A very weak signal at ~200 eV for alginate/chitosan blend coatings was assigned to Cl 2*p* and indicates chloride ions, as counterions.

As XPS needs to be performed in a high vacuum environment, the role of hydration water cannot be assessed by this technique. Accordingly, we studied hydrated samples by DRIFT. The DRIFT spectrum of amorphous CPC [Fig. 4 and 1] shows characteristic peaks from ~3000 to ~3400 cm^{-1} and a sharp peak at 1653 cm^{-1} indicative of a high water content sample. According to the model proposed by Posner *et al.*[44] describing the spherical structure of the amorphous calcium phosphate precursor, there are numerous water molecules between the individual calcium phosphate clusters. Such a structure containing much structural water is expected to be useful for obtaining better dispersion of particles within the hydrogel matrix. The hydroxyl peak at 3567 cm^{-1} is characteristic of CPC and the band at around 1457 cm^{-1} can be assigned to carbonate ions.[45]

All hydrogel coatings on silicon wafers, including composite coatings, alginate/chitosan coatings, and alginate or chitosan reference coatings, presented common IR absorbance bands. Each displayed a broad band at around 3400 cm^{-1} (hydroxyl stretch), indicative of high water uptake and hydrogen bonding, and an aliphatic C–H stretching band in the region 2931–2977 cm^{-1} (Fig. 4). However, the OH^- stretching vibration associated with the structure of CPC at 3567 cm^{-1} (Refs. 17, 45, and 46) disappeared in the composite coatings, indicating interaction of CPC with the hydrogel matrix through its abundant OH^- groups. This interaction might be beneficial for promoting the dispersion of CPC particles in the hydrogel matrix, as observed in the TEM images.

A peak at 1732 cm^{-1} in alginate samples was assigned to free COOH groups,[47] while the bands at 1611 and 1409 cm^{-1} were attributed to the antisymmetric and symmetric stretches of COO^- carboxylate salt groups[48,49] [Fig. 4].

The spectrum of chitosan showed an amide I band at 1657 cm^{-1} [Fig. 4 and 5].[48] The vibrational absorbance at 1591 cm^{-1} was assigned to the amino band (N–H) (Ref. 48) while 1376 cm^{-1} was attributed to the –C–O– stretching mode of the primary alcohol group (CH_2–OH) (Ref. 50) in chitosan.

The IR region from 1700 to 1300 cm^{-1} was similar for the composite coatings and the alginate/chitosan blend coatings, with broad bands at 1608 and 1419 cm^{-1}. The band at 1608 cm^{-1} is attributed to an overlap of the COO^- antisymmetric stretch in alginate and of N–H bands from chitosan.[51,52] The peak at around 1419 cm^{-1} was assigned to the COO^- symmetric stretch in alginate interacting with the NH_3^+ group of chitosan.[53]

Thus, CPC powders contain some HA, as indicated by the observed peak at 3567 cm^{-1}.[17,45,46] The disappearance of this peak in composite coatings implies that the CPC interacts with the organic hydrogel through its hydroxyl groups. In addition, this IR analysis shows that the electrostatic interactions between alginate and chitosan observed in alginate/chitosan hydrogels persisted in the composite coatings.

D. Release of FD 70 from composite coatings on silicon wafers

In this study we chose to use FITC-labeled dextran as a model water-soluble macromolecule. The FITC label enabled convenient assessment. In this study, it was not of interest

whether the FITC label affects the release rate compared with unlabeled dextran; if such hydrogel coatings are to be used with a specific dopant such as a growth factor, it is necessary anyway to measure its release rate. In this study, we aimed to determine the release kinetics for FD 70 such as to obtain an indication of the order of times of release for a diffusant of MW 70 kDa, which would be useful as a guide for subsequent studies with specific biomacromolecules.

The release of FD 70 from hydrogel coatings with and without calcium phosphate nanoparticles was studied by fluorescence assays, with a calibrated standard curve. The Jonckheere-Terstra test[38] indicated that the release of FD 70 from composite coatings with 0.3% CPC had almost the same profile as the release from pure alginate/chitosan blend coatings (the latter has been reported in Ref. 9), as shown in Fig. 5. However, a significantly higher release rate was observed when the CPC content was 0.5% or higher. The release difference between the composite coatings containing 0.5% and 1.0% CPCs was relatively small compared to that of the composite coatings containing 0.3% CPC. This is similar to the change of roughness measured by AFM, where the composite coatings with 0.3% CPC had almost the same roughness as the undoped hydrogel coatings.

Although dual phase kinetics was used to fit the experimental release data for the alginate/chitosan hydrogel coatings, it was not possible to obtain a good fit of the observed release behavior to commonly used Korsmeyer-Peppas models for the composite coatings, indicating more complex release behavior of our composite coatings. The release kinetics might be affected by a complex superposition of various effects such as swelling of the hydrogel matrix, release of calcium ions affecting alginate cross-linking, and volume changes as the CPC dissolves. The release rate (regression coefficient) decreased gradually with time for all composite coatings with different contents of CPC, but it cannot be fitted to first order kinetics.[54] In order to obtain release rate coefficients, different parts of the curves were fitted to a zero order release kinetics model.[55]

$$\frac{(M_t - M_L)}{(M_\infty - M_L)} = k \cdot (t - t_L), \tag{1}$$

where M_t and M_∞ are the released amount at time t and the overall released amount, respectively, M_L is the released amount at time t_L when the zero order release model begins, k is a release constant.

The release from composite coatings after 2 min for 0.3% CPC and after 10 min for both 0.5% CPC and 1.0% CPC appeared to be better described by double or triple phase zero order release kinetics, as shown in Fig. 6. The acceptability of the release model fit was tested by ANOVA based on linear regression analysis as shown in Table II for 0.3% CPC. Similarly, release data from 0.5% and 1.0% CPC hydrogel coatings all showed a zero significant value of F at a level of 0.05. The gradual decrease in release arose from the depletion of FD 70 within the composite coatings accompanying the release over time, and thus a decreased entropic driving force. It is worth noting that the linear kinetics model does not fit very well with the experiment data for the composite coatings with 1% CPC after 47 min, although it is the best fit among the available less complex models. As discussed before, the complex superposition of various effects have complicated the release kinetics.

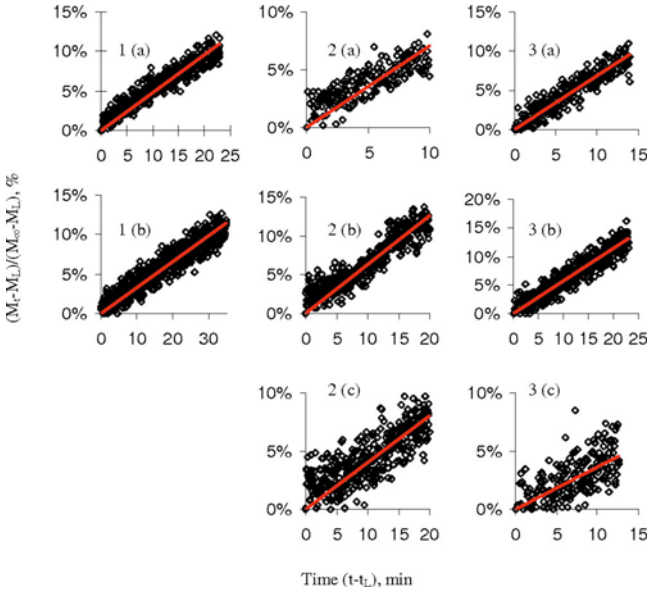

FIG. 6. Release kinetics of FD 70 into SBF from composite coatings containing different percentages of CPC powders, on silicon wafers; (1) 0.3% CPC, (a) 2–25 min and (b) 25–60 min; (2) 0.5% CPC, (a) 10–20 min, (b) 20–40 min, and (c) 40–60 min; (3) 1.0% CPC, (a) 10–24 min, (b) 24–47 min, and (c) 47–60 min.

E. Release of FD 70 from alginate/chitosan blend coatings on electrochemically deposited CaP coatings on titanium

The release profile of FD 70 into SBF from alginate/chitosan blend coatings deposited onto a calcium phosphate base layer on Ti substrate is shown in Fig. 7. This release behavior is similar to that observed on paper substrates[43] but with a lower overall release percentage. The similar release kinetics compared to coatings on paper may arise from the rough surface area of calcium phosphate coatings on Ti (rms=300 nm),[20] noting that the paper substrate likewise provides a rough substrate topography akin to that of commercial hydroxyapatite coatings. The release percentage was 48% at 20 min, which was two-thirds of the corresponding release percentage on the paper substrates, 74%.

F. Release of calcium and phosphate ions

The release of calcium and phosphate ions was analyzed by ICP-OES. It was found that for times shorter than 20 h, the additional amounts of calcium and phosphate supplied by release were too low to be detectable by this technique against the high background of these ions in SBF. As shown in Fig. 8, measurable amounts of calcium and phosphate ions were released from the alginate/chitosan/CPC composite coatings over a period of 3 d at *p*H 7.2. After 3 d, the release became immeasurably small over the subsequent 24 days.

TABLE II. ANOVA analysis of release model fit for the release of FD 70 from composite coatings with 0.3% CPC powder on Si wafers in SBF. (a and b denote the time segments of between 2 and 25 min and between 25 and 60 min, respectively.)

Predictor	Dependent variable	Regression coefficient k		R		R square	
		a	b	a	b	a	b
t-t_L	$\frac{M_t-M_L}{M_\infty-M_L}$	0.005	0.003	0.988	0.987	0.976	0.974

Source of variance	Sum ofsquares		df		Mean square		F [a]	
	a	b	a	b	a	b	a	b
Regression	1.872	2.990	1	1	1.872	2.990	Value 19 110.904	262 42.544
Residual	0.045	0.079	460	693	0.000	0.000	Sig. 0.000	0.000
Total	1.918	3.069	461	694				

[a]At the 0.05 level.

After 27 d the *pH* was lowered to 6.0 in order to determine whether there was any CPC left in the hydrogel coating. The basis for this is that the release of calcium and phosphate ions is increased at *p*H 6 as the solubility of calcium phosphates increases with decreasing *p*H.[56] Similarly, calcium and phosphate ions were released from the underlying calcium phosphate layer of alginate/chitosan/CaP layered coatings over a period of 3 days at *p*H 7.2. Decreasing the *p*H to 6.0 also led to additional release of calcium and phosphate ions in this structure (Fig. 9).

IV. DISCUSSION

The release of biomacromolecules from hydrogel coatings offers a means of localized control of biological processes adjacent to an implant surface,[2–8] and hydrogel coatings comprising alginate or chitosan have been investigated by a number of researchers for their use in this application.[21–34] On the other hand, a thin release coating provides a limited reservoir, and release may be effective only over a short period of time. The kinetics of release depend markedly on effects such as cross-linking and swelling of the hydrogel. As the structure and properties of alginate are affected by the concentration of calcium ions, the question arose whether the release of biomacromolecules from an alginate based hydrogel coating would be affected by a calcium rich environment, provided either by codispersed calcium phosphate nanoparticles or by an underlying calcium phosphate coating. The elution of fluorescently labeled dextran (FD) probe molecules from alginate/chitosan hydrogel coatings was reported earlier,[9] and in this study we aimed to see if there would be significant changes upon addition of the calcium phosphate in either variant.

The two coating designs represent possible usages wherein both macromolecules and calcium and phosphate ions are desired to be available to the biological milieu adjacent to an implant. A thin hydrogel coating loaded with macromolecules such as growth factors on top of a hydroxyapatite (HA) coating is a scenario for orthopaedic implants, whereas a coating comprising biomacromolecules and dispersed calcium phosphate nanoparticles may be of value for orthopaedic implants that do not contain a HA layer. For both scenarios, it is important to define possibilities and limitations for applications from knowledge of a number of properties, including release rates, loadings, and physical properties of the coatings. In this study we aimed to scope data on physical properties and release kinetics and durations.

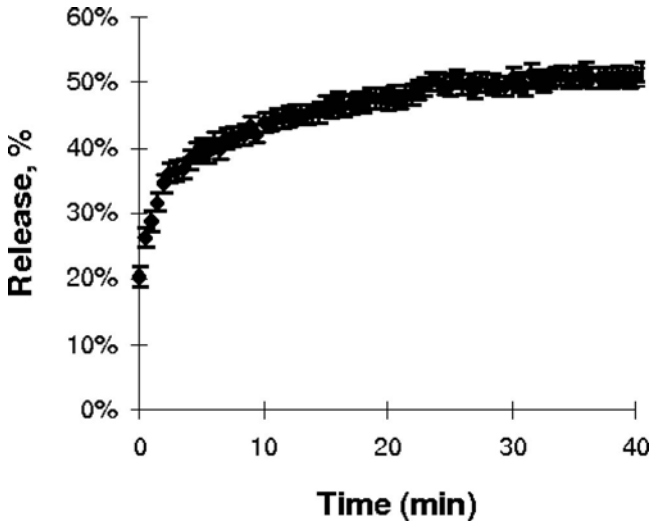

FIG. 7. Release of FD 70 from alginate/chitosan/CaP layered coatings on titanium into SBF.

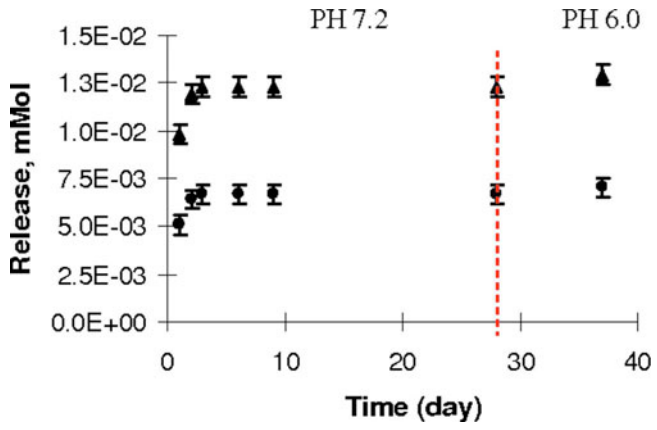

FIG. 8. Release of calcium (▲) and phosphate (●) ions from composite coatings on paper substrate, measured by ICP-OES.

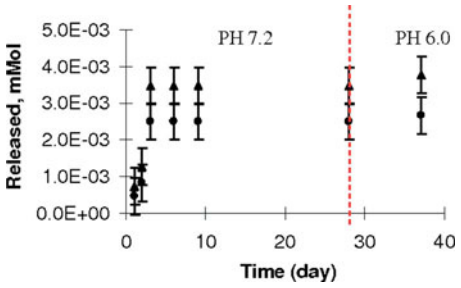

FIG. 9. Release of calcium (▲) and phosphate (●) ions from alginate/chitosan/CaP layered coatings on titanium, measured by ICP-OES.

The release of FD represents, of course, only a model system that we chose to use to probe for calcium effects on the release of a particular eluant. In practical applications, the actual release kinetics of a specific bioactive macromolecule would have to be determined by measurements; our data provide only an order of magnitude frame for molecules with similar MWs as those of the FDs used.

A key consideration comprises the physical properties of the hydrogel coatings. As surface roughness is well known to affect the cellular and tissue responses, it was important to ascertain whether the incorporation of CPC nanoparticles would substantially affect the surface topography. Clearly, our SEM and AFM data show that there is an increase in the surface roughness (rms values), but the increases are much smaller than the topographical features used in many studies to influence cell responses to surface topography. The hydrogel/CPC composite coatings generally have the same smooth structure as undoped alginate/chitosan layers, with the most frequently detected peak height of the composite coatings below 30 nm. Thus, we can conclude that the surface topography of the coatings is not a biologically relevant factor when comparing the pure hydrogel coatings and CPC-loaded coatings. This allows the composite coating to be considered as an approximate slab/monolithic model, analogous to the blend coating.[9]

The smallness of the effect of nanoparticle incorporation upon topography is related to the good dispersion of the nanoparticles. As our TEM images show, the nanoparticles we used are well dispersed; while some aggregation can be observed, there are no large clumps that would protrude markedly from the coating. XPS also shows that the nanoparticles are covered by a layer of hydrogel; thus, cells would not be exposed to CPC surface regions.

These analytical studies suggest that the coatings may present biointerfacial properties akin to those of undoped alginate/chitosan hydrogels. The data we collected contain no adverse indication regarding use on implants. Thus, a more important factor for consideration for possible applications may be the release kinetics achievable with these two coating structures.

The release of macromolecules is feasible from such structures, but occurs over very short time frames with a burst release behavior. The time frames are overall similar to those recorded with FD doped alginate/chitosan coatings without any additional bulk calcium phosphate present,[9] but the fact that the observed release kinetics do not fit established release kinetics descriptions over the entire period indicates that the situation is quite complex. The mechanism of outdiffusion driven by a concentration gradient is not the only determinant; there appear to be time-dependent superimposed phenomena such as swelling of the hydrogel matrix, release of calcium ions affecting alginate cross-linking, and volume changes as the CPC dissolves, that affect the observed elution of the FD probe molecules. We also note that increased calcium concentration leads to a faster rate of release. The details of the various factors such as swelling are in need of further study before a more detailed interpretation of the observed release kinetics is feasible. Fitting of the experimental data to multistep models is not particularly instructive; there are so many parameters that a number of fits give similar quality of fitting, and the physical basis is not available to assess how meaningful they are.

The release of calcium and phosphate ions takes place over longer time frames than the elution of FD, but after 3 d the amounts eluting have become very small, even though the later lowering of the solution *p*H shows that there is still payload left for elution. It is interesting that the time frames are similar for elution of calcium and phosphate ions for the two structures comprising nanoparticles dispersed within the hydrogel coating and a CaP layer underneath the hydrogel layer. However, in both cases the release times appear to be too short to be viable for assisting in longer-term bone regeneration. Whether the short-term release of calcium and phosphate ions has therapeutic benefits in the early stages of implant integration remains to be determined.

Thus, our data show that it is feasible to deliver both macromolecular payload and calcium and phosphate ions concurrently from either of the two structures investigated, but only over relatively short time frames. When CPC powder is mixed into the hydrogel coating, it releases calcium and phosphate ions and does not significantly interfere with the release of FITC-dextran. On the other hand, calcium and phosphate ions can be delivered by diffusion from a CaP layer applied underneath a hydrogel layer, and again the concurrent release of macromolecules is little affected. Calcium ions do, however, affect the hydrogel structure somewhat, and time-dependent changes in the density and cross-linking of the hydrogel lead to complex release kinetics.

V. CONCLUSIONS

Biomacromolecules and calcium and phosphate ions can be released concurrently from either of two structures: a composite coating containing both macromolecules and CPC within an alginate/chitosan hydrogel matrix, or a macromolecule-doped hydrogel coating on top of a calcium phosphate layer. The release kinetics of the macromolecules is similar to that observed earlier without CaP present, indicating that the additional presence of these particles or layer does not substantially affect the release of the probe molecules from the hydrogel, although at higher concentrations some change is observed, which is likely due to the calcium

ion concentration affecting the structure of the alginate/chitosan gel. The release of FD 70 from composite coatings with different CPC percentages, from 0.3% to 1.0%, was better described by double or triple phase zero order release kinetics. The release kinetics thus show a complex time dependence that indicates that in addition to outdiffusion, there are other, time-dependent factors such as swelling of the gel. This is not surprising in light of the known effects of calcium ions on alginate.

The similarity of release behaviors with different CPC nanoparticle concentrations is accompanied by an absence of substantial changes in the physical appearance of the coatings. The surface topography does not increase substantially, and the nanoparticles appear to be well embedded within the hydrogel matrix.

ACKNOWLEDGMENTS

This study was supported partly by an International Postgraduate Research Scholarship and a University of South Australia Postgraduate Award to Ms. Ping Peng, and by the Australian Research Council under the Special Research Centres Scheme (SRC for Particle and Material Interfaces).

[1]B. D. Ratner, J. Mol. Recognit. **9**, 617 (1996).
[2]D. A. Puleo and A. Nanci, Biomaterials **20**, 2311 (1999).
[3]Y. Nakayama, J. Kim, S. Nishi, H. Ueno, and T. Matsuda, J. Biomed. Mater. Res. **57**, 559 (2001).
[4]L. Rowan, P.W. Stratford, A.S. Taylor, and T.A. Vick, WO Patent No. 2001001957 (11 Jan 2001).
[5]J. Stamler, J. Loscalzo, and J.D. Folts, U.S. Patent No. 6255277 (3 July 2001).
[6]A. B. Anderson, Med. Device Technol. **14**, 16 (2003).
[7]H. W. Kim, J. C. Knowles, and H. E. Kim, J. Mater. Sci. Mater. Med. **16**, 189 (2005).
[8]B. Lagerqvist, S. K. James, U. Stenestrand, J. Lindback, T. Nilsson, and L. Wallentin, N. Engl. J. Med. **356**, 1009 (2007).
[9]P. Peng, N. H. Voelcker, S. Kumar, and H. J. Griesser, BioInterphases **2**, 95 (2007).
[10]K. Soballe, Acta Orthop. Scand. **64**, 1 (1993).
[11]F. Barrere, C. M. van der Valk, R. A. J. Dalmeijer, C. A. van Blitterswijk, K. de Groot, and P. Layrolle, J. Biomed. Mater. Res., Part B: Appl. Biomater. **64A**, 378 (2003).
[12]P. Habibovic, C.M. van der Valk, K. De Groot, and P. Layrolle, Key Eng. Mater. **240–242**, 387 (2003).
[13]S. Langstaff, M. Sayer, T. J. N. Smith, and S. M. Pugh, Biomaterials **22**, 135 (2001).
[14]C. P. Klein, P. Patka, J. G. Wolke, J. M. de Blieck-Hogervorst, and K. de Groot, Biomaterials **15**, 146 (1994).
[15]C. J. Damien and J. R. Parsons, J. Biomed. Mater. Res., Part B: Appl. Biomater. **2**, 187 (1991).
[16]T. Matsumoto, M. Okazaki, M. Inoue, S. Ode, C. Chang-Chien, H. Nakao, Y. Hamada, and J. Takahashi, J. Biomed. Mater. Res. **60**, 651 (2002).
[17]K. C. Blakeslee, A. Robert, and S. R. Condrate, J. Am. Ceram. Soc. **54**, 559 (1971).
[18]C. Rey, B. Collins, T. Goehl, I. R. Dickson, and M. J. Glimcher, Calcif. Tissue Int. **45**, 157 (1989).
[19]J. E. Barralet, S. M. Best, and W. Bonfield, Biomed. Mater. Eng. **6**, 101 (1996).
[20]P. Peng, S. Kumar, N. H. Voelcker, E. Szili, R. S. C. Smart, and H. J. Griesser, J. Biomed. Mater. Res., Part A **76A**, 347 (2006).
[21]M. D. Weir, H. H. K. Xu, and C. G. Simon, J. Biomed. Mater. Res., Part A **77A**, 487 (2006).
[22]D. W. Green, S. Mann, and R. O. C. Oreffo, Soft Matter **2**, 732 (2006).
[23]G. Fuentes, M. Gonzalez, G. Perez, J. A. Delgado, E. Peon, M. L. Rojas, J. Casquero, and P. Miranda, Lat. Am. Appl. Res. **35**, 289 (2005).
[24]S. Tajima, N. Nishimoto, Y. Kishi, S. Matsuya, and K. Ishikawa, Dent. Mater. J. **23**, 329 (2004).
[25]M. Sivakumar and K. P. Rao, J. Biomed. Mater. Res., Part A **65A**, 222 (2003).
[26]I. Lévêque, K. H. Rhodes, and S. Mann, J. Mater. Chem. **12**, 2178 (2002).
[27]M. Takechi, Y. Miyamoto, K. Ishikawa, T. Toh, T. Yuasa, M. Nagayama, and K. Suzuki, Biomaterials **19**, 2057 (1998).
[28]X. P. Wang, L. Chen, H. Xiang, and J. D. Ye, J. Biomed. Mater. Res., Part B: Appl. Biomater. **81B**, 410 (2007).
[29]S. M. Kuo, S. J. Chang, T. W. Chen, and T. C. Kuan, J. Biomed. Mater. Res., Part A **76A**, 408 (2006).
[30]T. Dvir, O. Tsurgang, and S. Cohen, Isr. J. Chem. **45**, 487 (2005).
[31]Z. S. Li, H. R. Ramay, K. D. Hauch, D. M. Xiao, and M. Q. Zhang, Biomaterials **26**, 3919 (2005).
[32]D. W. Hutmacher, J. C. H. Goh, and S. H. Teoh, Ann. Acad. Med. Singapore **30**, 183 (2001).
[33]S. Itoh, I. Yamaguchi, M. Suzuki, S. Ichinose, K. Takakuda, H. Kobayashi, K. Shinomiya, and J. Tanaka, Brain Res. **993**, 111 (2003).
[34]H. Milhofer-Furedi, P. Bar Yosef Ofir, M. Sikirin, C. Gergely, and F. Cuisinier, WO Patent No. 2004047880 (10 June 2004).
[35]D. M. Price, M. Reading, and T. J. Lever, J. Therm Anal. Calorim. **56**, 673 (1999).
[36]J. R. Adams and N. M. Bashara, Surf. Sci. **47**, 655 (1975).
[37]J. Vörös, Biophys. J. **87**, 553 (2004).
[38]LEAD Technologies, SPPS@Base system, LEAD Technologies Inc., 2002.
[39]SPSS, Regression, 2004.
[40]J. Leckenby, D. Faddis, and G. Hsiao, Combined thermal, mechanical, and morphological characterization of polymers on a nanometer spatial scale. 1999 (cited 6 July 2004). Available from http://www.iscpubs.com/articles/al/a9904lec.pdf
[41]H. M. Pollock and A. Hammiche, J. Phys. D: Appl. Phys. **34**, R23 (2001).
[42]D. M. Price, M. Reading, A. Caswell, A. Hammiche, and H. M. Pollock, Microscopy and Analysis **65**, 17 (1998).
[43]P. Peng, Ph.D. thesis, University of South Australia, 2005.
[44]A. S. Posner, N. C. Blumenthal, and F. Betts, *Chemistry and Structure of Precipitated Hydroxyapatites* (Springer-Verlag, Berlin, Heidelberg, 1984), pp. P155–P171.
[45]M. Shirkhanzadeh, J. Mater. Sci. Lett. **12**, 16 (1993).
[46]S. Rossler, A. Sewing, M. Stolzel, R. Born, D. Scharnweber, M. Dard, and H. Worch, J. Biomed. Mater. Res., Part B: Appl. Biomater **64**, 655 (2002).
[47]R. A. A. Muzzarelli, *Natural Chelating Polymers* (Pergamon, Oxford, 1937), p. 256.
[48]S. Kim, Y. Kim, J. Jegal, G. Lim, and K. Lee, J. Appl. Polym. Sci. **85**, 714 (2002).
[49]R. Valentin, R. Horga, B. Bonelli, E. Garrone, F.D. Renzo, and F. Quignard, Biomacromolecules **7**, 877 (2006).
[50]R. Murugan and S. Ramakrishna, Biomaterials **25**, 3829 (2004).
[51]X. Yan, E. Khor, and L. Lim, J. Biomed. Mater. Res., Part B: Appl. Biomater. **58**, 358 (2001).
[52]X. Yan, E. Khor, and L. Lim, Chem. Pharm. Bull. (Tokyo) **48**, 941 (2000).
[53]G. Lawrie, I. Keen, A. Chandler-Temple, B. Drew, P. Fredericks, and L. Grøndahl, Biomacromolecules **8**, 2533 (2007).
[54]P. Costa and J. M. S. Lobo, Eur. J. Pharm. Sci. **13**, 123 (2001).
[55]N. A. Peppas, Pharm. Acta Helv. **60**, 110 (1985).
[56]G. Willmann, Adv. Eng. Mater. **1**, 95 (1999).